Quantum Electronics **48** (3) 244–250 (2018)

https://doi.org/10.1070/QEL16567

Effect of absorbing coating on ablation of diamond by IR laser pulses

T.V. Kononenko, P.A. Pivovarov, A.A. Khomich, R.A. Khmelnitskii, V.I. Konov

Abstract. **We study the possibility of increasing the efficiency and quality of laser ablation microprocessing of diamond by preliminary forming an absorbing layer on its surface. The laser pulses having a duration of 1 ps and 10 ns at a wavelength of 1030 nm irradiate the polycrystalline diamond surface coated by a thin layer of titanium or graphite. We analyse the dynamics of the growth of the crater depth as a function of the number of pulses and the change in optical transmission of the ablated surface. It is found that under irradiation by picosecond pulses the preliminary graphitisation allows one to avoid the laser-induced damage of the internal diamond volume until the appearance of a self-maintained graphitised layer. The absorbing coating (both graphite and titanium) much stronger affects ablation by nanosecond pulses, since it reduces the ablation threshold by more than an order of magnitude and allows full elimination of a laser-induced damage of deep regions of diamond and uncontrolled explosive ablation in the near-surface layer.**

Keywords: *laser ablation, microstructuring, diamond, absorbing coating.*

1. Introduction

Many potential applications of synthesised diamonds, including the fabrication of diamond elements for optics and photonics, microelectromechanical systems, biochemical reactors, sensors, field emitters, etc., require a perfect technology of surface microstructuring. During the last two decades several efficient solutions of this problem have been proposed and successfully implemented, including the silicon replica method [1, 2], reactive ion etching [3–5], etching in the inductively coupled plasma [6–8], and laser ablation [9–15]. One of the advantages of the latter technique is that it is a single-step process, which is commonly performed in air, provides the formation of arbitrary spatial shapes and is easily adaptable to a new task. The drawbacks of laser processing are the lower spatial resolution and higher roughness of the resulting surface, as compared to the results obtained using the above alternative methods.

Diamond is a wide-band (5.45 eV) dielectric and, therefore, in the first experiments on the diamond surface laser microstructuring ultraviolet excimer lasers were used [16–19]. In these experiments, it was found that laser ablation of diamond is accompanied by the appearance of a thin self-maintained graphitised layer on its surface, providing efficient absorption of laser radiation at any wavelength [20]. Due to this effect, nanosecond pulses of IR and visible spectral range (λ = 532–1064 nm), weakly absorbed in diamond at high energy densities but capable of initiating optical breakdown (graphitisation), can be used to cut diamond, including industrial applications. However, attempts to use such pulses for profiling the diamond surface turned out unsuccessful (see, e.g., [9]) because of the formation of multiple cracks in the volume of the exposed material and large caverns on its surface.

A much better quality of the diamond surface processing was demonstrated by ultrashort (femtosecond and picosecond) pulses of IR and visible range [9–13], the interest to which permanently grows during the last decade. An important reason for the popularity of ultrashort pulses is the essential progress of recent years in the development of appropriate laser sources that led to the assortment widening, the reliability improvement, and the increase in such key parameters as the mean power and the pulse repetition rate by a few orders of magnitude. All these factors allow a breakthrough in the productivity of precision laser processing and open a way to practical exploitation of specific regimes of diamond processing, e.g., nanoablation [4, 15], characterised by ultralow (below 10^{-3} nm per pulse) rates of material removal.

It is worth noting that although the use of ultrashort pulses strongly enhances the precision of the diamond surface processing and considerably reduces the degree of damaging the inner regions as compared to the results of nanosecond pulse irradiation, it does not solve the problem in principle. Before the appearance of a surface graphitised layer, the efficient absorption of laser radiation in diamond is possible only due to the complex process of nonlinear ionisation of the

T.V. Kononenko, V.I. Konov A.M. Prokhorov General Physics Institute, Russian Academy of Sciences, ul. Vavilova 38, 119991 Moscow, Russia; National Research Nuclear University 'MEPhI', Kashirskoe shosse 31, 115409 Moscow, Russia; e-mail: kononen@nsc.gpi.ru;
P.A. Pivovarov A.M. Prokhorov General Physics Institute, Russian Academy of Sciences, ul. Vavilova 38, 119991 Moscow, Russia;
A.A. Khomich A.M. Prokhorov General Physics Institute, Russian Academy of Sciences, ul. Vavilova 38, 119991 Moscow, Russia; V.A. Kotelnikov Institute of Radio Engineering and Electronics (Fryazino Branch), Russian Academy of Sciences, pl. Akad. Vvedenskogo 1, 141190 Fryazino, Moscow region, Russia;
R.A. Khmelnitskii A.M. Prokhorov General Physics Institute, Russian Academy of Sciences, ul. Vavilova 38, 119991 Moscow, Russia; V.A. Kotelnikov Institute of Radio Engineering and Electronics (Fryazino Branch), Russian Academy of Sciences, pl. Akad. Vvedenskogo 1, 141190 Fryazino, Moscow region, Russia; P.N. Lebedev Physical Institute, Russian Academy of Sciences, Leninsky prosp. 53 , Moscow, Russia 119991; Troitsk Institute for Innovation and Fusion Research (TRINITI), ul. Pushkovykh 12, Troitsk, 142190 Moscow, Russia

Received 7 November 2017
Kvantovaya Elektronika **48** (3) 244–250 (2018)
Translated by V.L. Derbov

material, which depends on the local radiation intensity, as well as on the presence of different structural defects. In particular, this leads to a significant spread in the results of measuring the optical breakdown threshold in diamond [21]. As a result, the zone of radiation absorption and consequent intense heat release can be located not only at the surface, but also deep in the material volume, which leads to its optical breakdown (damage). The optical breakdown in the diamond volume is accompanied by the appearance of a microscopic graphitised region capable of efficient absorption of the incident light and generation of strong tensile stresses in the surrounding material, leading to the appearance of microscopic cracks [22]. Obviously, the appearance of such defects in the volume of the processed material rather negatively affects the characteristics of the fabricated diamond microstructure, particularly if it is planned to transmit radiation through it.

The focusing of a laser beam onto the sample surface commonly does not provide localisation of absorption of laser radiation in the thin surface layer. The reason it that a considerable decrease in laser intensity occurs only deeper than the Rayleigh length $z_R = \pi n w^2/\lambda$, where $w = 2\lambda f/(\pi D)$; $n = 2.4$ is the refractive index of diamond; λ is the wavelength; f is the focal length; and D is the beam diameter at the lens. For example, in the typical case of diamond surface microstructuring with IR pulses ($\lambda = 1.03$ μm) by means of a standard galvanometer scanner ($f = 160$ mm, $D = 10$ mm), the Rayleigh length amounts to about 800 μm, which is comparable with the typical thickness of commercially available plates of polycrystalline diamond. One should keep in mind that the number of pulses necessary to initiate the formation of a self-maintaining graphitised layer and the beginning of surface ablation is reduced with the growth of the incident energy density, which is a manifestation of the 'incubation effect' [22]. Using a sufficiently high energy density, the graphitised layer can be produced by the first pulse. However, a question arises, whether the graphitised layer possesses sufficiently low transmission to decrease the intensity of laser radiation penetrating through it to the level that excludes the optical breakdown in the process of subsequent ablation.

A possible solution to this problem is the preliminary deposition of a thin coating of a strongly absorbing material on the surface of the processed diamond plate. Potentially, this coating can localise the absorption of laser radiation at the surface of the sample from the very beginning of irradiation, accelerate the formation of a self-maintaining graphitised layer on the surface of diamond, or even decrease the minimal energy density necessary for its appearance.

The goal of the present experimental study was to check the above considerations and to clarify the influence of a strongly absorbing coating on the process of polycrystalline diamond ablation by picosecond ($\tau = 1$ ps) and nanosecond ($\tau = 10$ ns) pulses at a wavelength of 1030 nm. In the process of study, we tested two types of absorbing coatings, both a few hundred nanometres thick, namely, a titanium film and a graphite layer. Titanium is known for its good adhesion to diamond and low reflection coefficient, as compared to other metals, and the graphite layer can be obtained by phase modification of the surface of diamond itself. The complex study of the process of crater formation at the diamond surface included the measurements of the profile and the local transparency of the irradiated surface, as well as the investigation of the graphitised layer at the crater bottom by means of Raman spectroscopy.

2. Experiment

In the experiments, we used two 0.5-mm-thick plates measuring 10 mm × 10 mm cut from one optical-quality polycrystalline diamond grown using chemical vapour deposition (CVD). Both sides of the plates were mechanically polished and cleaned in an ultrasonic bath using acetone. Half the area of one of the plates was coated with a 300-nm-thick titanium film deposited using the method of vacuum evaporation. Into the other plate, the Ar^+ ions were implanted with the energy 250 keV and the doze 2×10^{15} cm^{-2} at room temperature. The damaged surface layer formed in this way was annealed in vacuum at the temperature 1400 °C during 1 hour and transformed into a layer of 280-nm-thick nanocrystalline graphite. Using the relation between the integral intensities of the peaks D (1367 cm^{-1}) and G (1595 cm^{-1}), selected from the Raman scattering spectrum, the mean size of graphite crystals in the produced absorbing layer was estimated to be $L_{cr} = 27$ nm [23].

Irradiation was performed by a VaryDisk50 multimode laser system (Dausinger+Giesen GmbH, Germany), generating pulses with the duration both 1 ps and 10 ns at the wavelength 1030 nm with the pulse repetition rate 200 kHz for the maximal mean power 20 W. The external Pockels cell locked with the laser provided the reduction of the repetition rate to 1 kHz and the formation of pulse trains of given length. Using a lens with $f = 100$ mm, the laser beam was focused into a spot with the diameter 23 μm at the 1/e level on the surface of the diamond plate mounted on the *xyz* micropositioner.

The diamond plates with metal and graphite coatings, as well as the uncoated area, were irradiated by a variable number of pico- and nanosecond pulses in the range of energy densities $F = 0.3-8$ J cm^{-2}. For each crater the 2D surface profile was obtained using a ZYGO NewView5000 white-light interferometer (ZYGO Corp., USA). Irradiating the uncoated diamond, we compared the local transmission of the material at the laser wavelength (1030 nm) before and after irradiation. To this end, the energy of probe pulses was reduced to the level excluding the diamond damage. The minimal energy density at the diamond surface that caused the fall of transmission after $N = 10^4$ laser pulses was accepted as the optical breakdown threshold. To record the Raman spectra at the bottom of the crater, we used a LamRam HR-800 microanalyser (HORIBA, Japan) equipped with an Ar^+ laser ($\lambda = 488$ nm).

3. Results

3.1. Ablation of uncoated diamond by picosecond pulses

A typical dependence of the crater depth on the number of laser pulses presented in Fig. 1 ($F = 1.2$ J cm^{-2}) allows one to conditionally distinguish three stages in the process of producing a deep crater in diamond. At the first stage ($N < 10$), the crater is not formed yet, which corresponds to a zero depth of the crater in the plot. At the second stage ($10 \leqslant N \leqslant 100$), the probability is great for the formation of an irregularly shaped crater with a bottom profile corresponding to a Gaussian distribution of energy in the laser beam and characterised by a large depth variation (or 'large spread of depths') (Fig. 2b). The latter fact determines the abnormally large value of the vertical error at the corresponding points of the crater depth dependence in Fig. 1. At the crater periphery, it is sometimes possible to find explicit microscopic cracks in

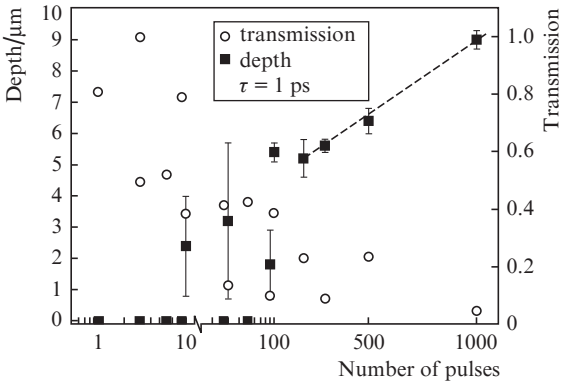

Figure 1. Dependence of the crater depth and local transmission of the material at the wavelength 1030 nm (the initial transmission equal to 1) on the number of pulses for uncoated diamond ablation by the pulses with the duration $\tau = 1$ ps ($F = 1.2$ J cm^{-2}).

diamond (Fig. 2a). And finally, the third stage ($N > 100$) is characterised by the presence of a bell-shaped crater (Figs 2c and 2d), and the increasing number of pulses leads to a linear growth of the crater depth, at least until the depth is much smaller than the crater diameter. An increase in the energy density in the laser spot is accompanied by the reduction of the first two stages. Thus, for the energy density $F = 1.2$ J cm^{-2} (Fig. 1) the third stage begins nearly after 100 pulses, and for $F = 8$ J cm^{-2} it takes only 10 pulses to achieve a linear growth of depth.

The characteristic morphology of the crater bottom (see Fig. 2a), formed at the second stage of irradiation, in combination with microscopic cracks, shows that their origin is due to the explosive mechanical destruction of the near-surface region of diamond. The most probable reason for this destruction is the tensile stresses in diamond that arise around one or a few graphite microinclusions, produced by the optical breakdown in the near-surface region. According to the collected experimental data, the thickness of the near-surface layer, inside which the optical breakdown can lead to the formation of a crater, does not exceed 5–6 μm. Besides the crater depth, Fig. 1 presents also the data on the variation of the transmission of laser pulses ($\lambda = 1030$ nm) in the irradiation spot, normalised so that the local transmission before the irradiation equals one. An important result is that a significant decrease in transmission is observed not only in the case of the surface crater formation, but also in the majority of the cases when the crater is yet absent (the first and the second stage). It is reasonable to suppose that this fall of transmission is caused by the optical breakdown relatively deep in the diamond, where the material cracking around the arising graphite microinclusions [22] does not lead to the formation of a surface crater.

Thus, during the first and the second stages, a single breakdown or multiple ones seem to occur inside the diamond at different depths within the laser caustic. The total duration of these stages is determined by the mean duration of the 'incubation period' [22] in the diamond for the used density of energy. However, the increased local concentration of structural defects in individual regions of the polycrystalline diamond is capable of significant acceleration of the creation of the conditions for the optical breakdown. In this case, it is statistically much more probable that such a defect region will appear beyond the thin near-surface layer. Apparently, this is

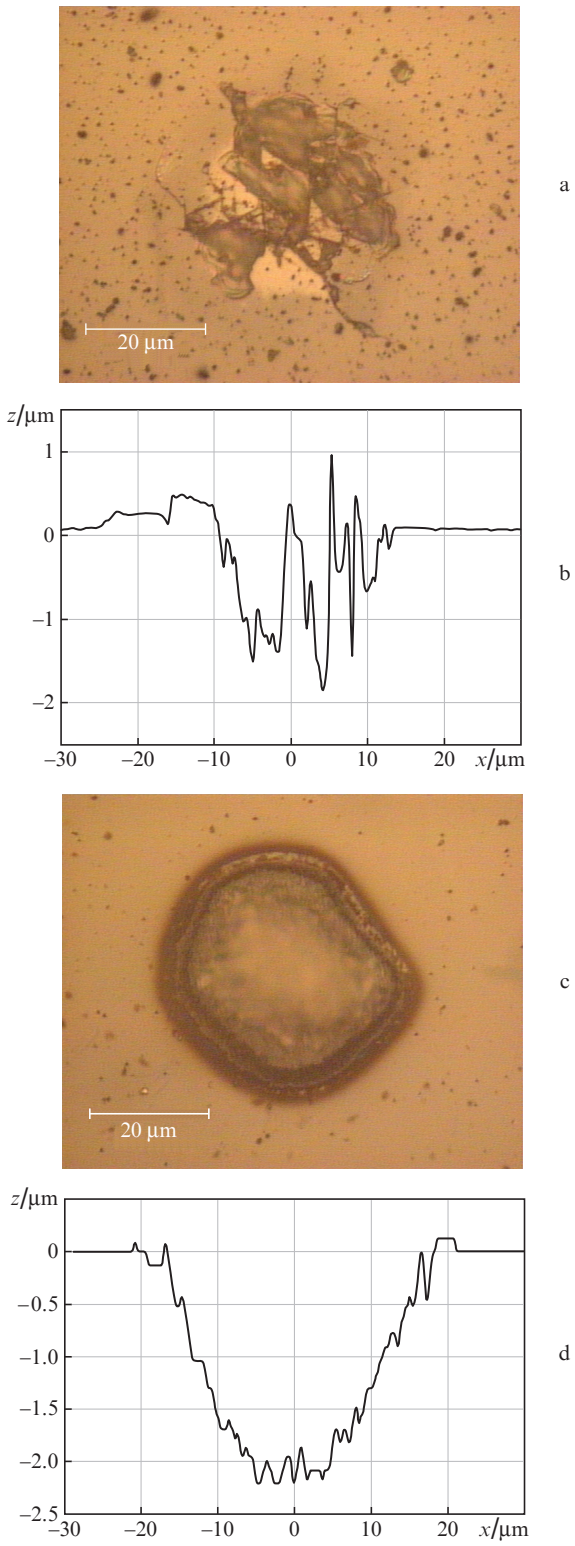

Figure 2. (a, c) Optical microscopic images and (b, d) surface profiles of typical craters, produced on the surface of uncoated diamond by pulses with the duration $\tau = 1$ ps ($F = 1.2$ J cm^{-2}): (a, b) crater of irregular shape and (c, d) bell-shaped crater.

the explanation of the fact that at the first stage the optical breakdown is not accompanied by the appearance of a crater at the surface.

When any kind of a crater is formed at the surface, its bottom appears to be covered with thin graphite layer, which is

confirmed by a change in the Raman spectrum (Fig. 3a), namely, the appearance of the peaks D (~ 1380 cm^{-1}) and G (~ 1570 cm^{-1}), characteristic for the sp^2-bound carbon [23]. As a rule, both peaks have a very large width and their ratio indicates a very high degree of the sp^2 phase amorphisation. A decrease in the diamond peak intensity (~ 1333 cm^{-1}) in the process of irradiation is due to an increase in the thickness of the laser-induced graphitised layer, which partially shields both the transmission of the exciting laser radiation into the sample, and the exit of the scattered radiation from the sample. Keeping in mind the relatively small difference between the wavelengths of the incident radiation and the scattered one and neglecting the reflection at the interfaces between the media, we can approximately estimate the graphitised layer transmission at the wavelength 488 nm (T_{gr}). To this end, we compare the intensity of the diamond peak at the bottom of the crater (I_{gr}) and in the initial diamond (I_{in}), namely, $I_{gr} = I_{in}T_{gr}^2$, and, therefore, $T_{gr} = (I_{gr}/I_{in})^{0.5}$.

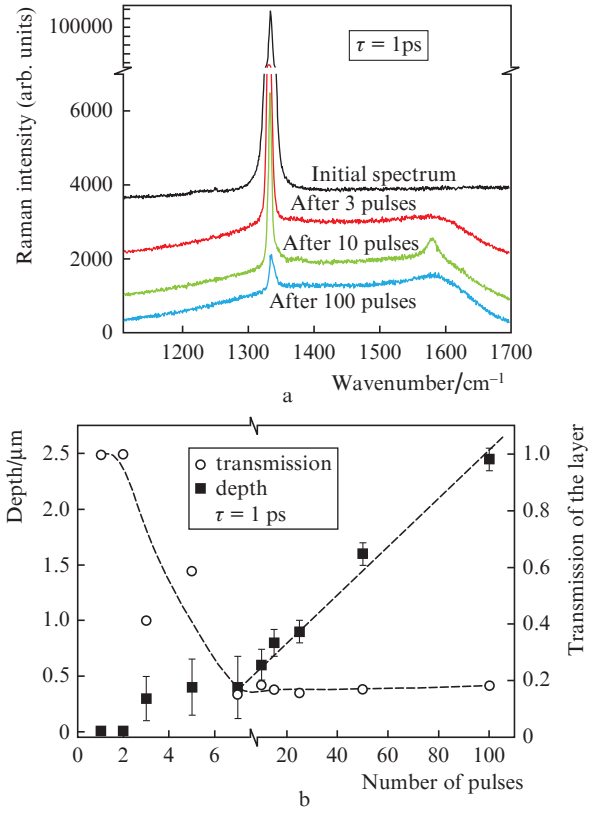

Figure 3. (a) Transformation of Raman spectrum with increasing number of pulses and (b) dependences of the crater depth and the transmission of the graphitised layer (λ = 488 nm) on the number of pulses for ablation of uncoated diamond by pulses with τ = 1 ps (F = 2.5 J cm^{-2}).

Typical dynamics of this parameter variation with the growth of the number of pulses is presented in Fig. 3b, where it is compared with the already known dependence of the crater depth. During the second stage of irradiation that is easily identified by the appearance of craters with a large spread of depths, the transmission of the graphitised layer decreases to ~ 0.2, which unambiguously confirms the growth of its thickness. At the linear section of the depth growth (the third stage of crater formation) the transmission remains virtually constant and, therefore, the thickness of the graphitised layer is almost unchanged. Using this fact, it is possible to assume that the transition from the random internal breakdowns to the steady-state surface graphitisation and ablation is determined exactly by the formation of a sufficiently thick self-maintaining graphitised layer, which provides the efficiency of the laser energy absorption at the surface, sufficient for the material evaporation.

To evaluate the thickness of the self-maintaining layer, we used the known data on the optical properties of nanocrystalline graphite (glassy carbon) [24,25], since the spectroscopic results show the closeness of this material to the graphitised layer. From the value of the imaginary part of the refractive index of the glassy carbon (k = 0.74) for the energy of quantum $h\nu$ = 2 eV, we calculated the absorption coefficient at the wavelength λ = 488 nm, $\alpha = 4\pi k/\lambda = 1.9 \times 10^5$ cm^{-1}. Then we found the stabilised thickness of the graphitised layer at T_{gr} = 0.2, $d_{gr} = -\ln(T_{gr})/\alpha$ = 85 nm. The obtained value agrees with the data presented in Ref. [20], according to which the thickness of the graphitised layer irradiated by femtosecond and picosecond pulses varies within the range 10–80 nm. Similarly one can evaluate the expected transmission of the graphitised layer for pulses having a duration of 1 ps (λ = 1030 nm): if k = 1.04 for $h\nu$ = 1 eV [24,25], then $\alpha = 1.27 \times 10^5$ cm^{-1} and, therefore, $T_{gr} = \exp(-\alpha d_{gr})$ = 0.34. Thus, the self-maintained graphitised layer provides a nearly threefold fall of the laser pulse intensity passing through it. Note that the estimated transmission of the graphitised layer considerably exceeds the previous results of measuring the diamond transmission for λ = 1030 nm at the stage of the linear growth of the crater depth (T_{gr} = 0.05–0.25, see Fig. 1). Obviously, in the latter case the measured quantity was integral transmission, affected not only by the transmission of the surface graphitised layer, but also by the absorption or scattering of laser radiation by the local graphite microinclusions and cracks, arising due to the optical breakdown in the volume of diamond.

3.2. Ablation of diamond with an absorbing coating by picosecond pulses

The deposition of a titanium film on the diamond surface did not considerably affect the process of crater formation by picosecond pulses. An obvious explanation is that the titanium layer 0.3 μm thick, as a rule, was completely removed already by the first laser pulse, and the observations by means of optical microscopy and Raman spectroscopy did not allow detection of any damage or modification of the opened diamond surface. The fact that at low energy densities (F < 1.3 J cm^{-2}) two-to-three pulses were necessary for the complete removal of the titanium film did not affect the final result anyway. The regularities of the subsequent irradiation (see Fig. 4a) completely corresponded to the above three-stage scenario including: 1) the absence of a crater and a graphitised layer at the diamond surface; 2) the formation of a shallow crater with strong modulation of the bottom profile and a simultaneous decrease in the transmission of the laser-induced graphitised layer to $T_{gr} \approx 0.2$; 3) the linear growth of the crater depth with the number of pulses with practically constant transmission of the graphitised layer. We emphasise that the total duration of the first and second stages in this case appeared to be almost the same as in the case of irradiating uncoated diamond (for the same incident energy density). This observation confirms the fact that there is no modification of the diamond surface, opened after the removal of the titanium coating.

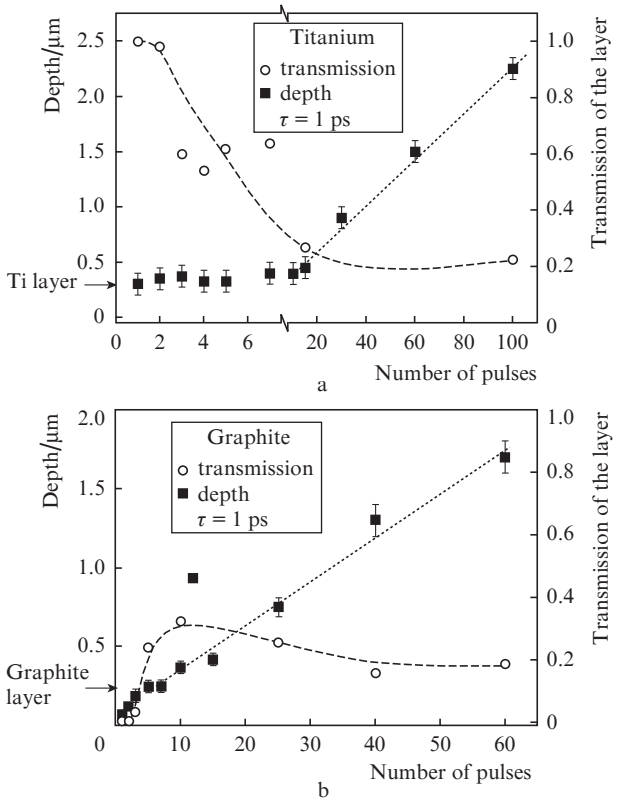

Figure 4. Dependences of the crater depth and the graphitised layer transmission (λ = 488 nm) on the number of pulses for the ablation of diamond with (a) titanium and (b) graphite coatings by the pulses with τ = 1 ps (F = 2.5 J cm^{-2}).

The initial transmission of the implanted graphite layer at the wavelength 488 nm is equal to zero (Fig. 4b). In the process of ablation, the transmission gradually grows and reaches ~0.35 in the maximum, when the crater depth becomes larger than the thickness of the implanted layer. This fact means that immediately after the removal of the implanted layer, the surface of the diamond appears to be covered by a laser-induced graphitised layer, although its transmission is somewhat greater than the level typical for deep craters (i.e., $T_{gr} \approx$ 0.2). Thus, the use of an implanted graphite layer eliminates the first stage of the crater formation, when the damage of inner regions of diamond is most probable. From the morphology of the studied craters, all of them having a bell-like shape, we concluded that the second stage is also absent in the present case, since the arising laser-induced graphitised layer hampers the optical breakdown in the near-surface layer. Although the graphitised layer requires a few tens of pulses for achieving the stable low level $T_{gr} \approx 0.2$, the dependence of the crater depth on the number of pulses is close to linear starting from the first pulse.

3.3. Ablation of diamond with an absorbing coating by nanosecond pulses

It is known that ablation of uncoated diamond by nanosecond pulses in the IR and visible range is determined by principally the same mechanisms and suffers from the same undesired consequences as irradiation of diamond by picosecond pulses, including the cracks appearing in the inner regions and the abnormally deep explosion caverns at the surface. The visible enhancement of the destructive action of laser radiation under the transition from picosecond pulses to nanosecond ones (see Ref. [9]) is explained mainly by an increase in the optical breakdown threshold and a corresponding increase in the minimal used energy densities. Due to this fact and the high threshold of the optical breakdown (F_{th} > 40 J cm^{-2}), which significantly exceeded the maximal values of the energy density, available with the chosen focusing optics, no investigation of the diamond ablation without a coating by pulses with τ = 10 ns was carried out.

The experiments on ablation of diamond with a titanium coating revealed a new and interesting feature. The first nanosecond pulse completely removes the metal layer not in the centre, but in the ring area at the periphery of the irradiated region (Fig. 5). In the central part of the laser spot, the first pulse causes only melting and partial evaporation of the metal film. Summarising the data for several pulse energies, we found that the full removal of the metal film by the first pulse occurs in the narrow range of energy densities 0.7 J cm^{-2} < F < 1.6 J cm^{-2}. However, the statistical analysis of the experimental data shows that there is an almost 5% probability that the metal will be removed simultaneously in the centre and at the periphery of the laser spot, i.e., the condition F < 1.6 J cm^{-2} is not valid. At present, we can only suppose that the mechanism of this full removal of the metal film (without damaging underlying diamond) by a single nanosecond pulse in the restricted range of energy densities is related to laser-induced thermoelastic stresses arising in the film.

The diamond surface opened after the first pulse looks undamaged not only immediately after the event, but also during the entire period of subsequent irradiation, in our case

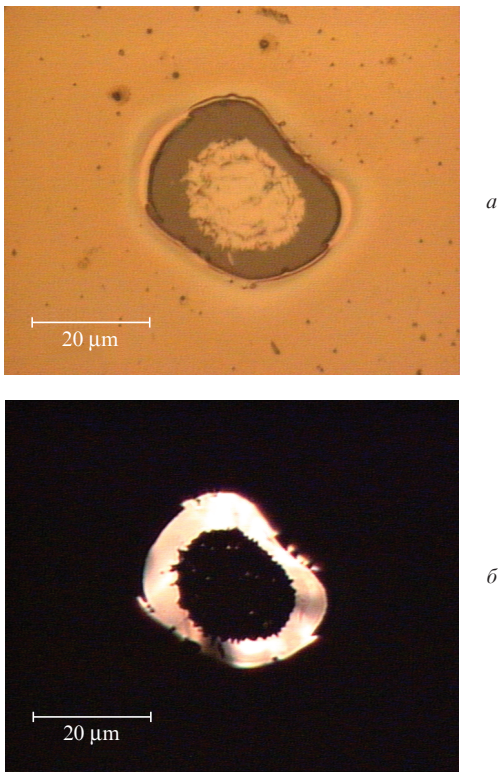

а

б

Figure 5. Images obtained by an optical microscope in (a) reflected and (b) transmitted light for the results of irradiating titanium-coated diamond by a single pulse with τ = 10 ns (F = 4.2 J cm^{-2}).

restricted to 100 pulses. For the total removal of metal in the central spot, a few laser pulses are required, and the surface of diamond free of metal appears to be coated by a graphitised layer, which is confirmed by the Raman spectra of the crater bottom. The transmission of the graphitised layer immediately after the removal of the metal coating becomes established at the level 0.1–0.15 and then only slightly varies in this range (Fig. 6a). Intense melting of metal in the central spot leads to the formation of 'waves' on its surface, comparable in height with the residual thickness of the film. The 'waves' are 'transferred' in the process of ablation to the graphitised surface of diamond. Further deepening of the crater does not lead to a noticeable growth of the surface roughness at the crater bottom.

In ablation of diamond with an implanted graphite layer by nanosecond pulses, the linear growth of the crater depth is observed from the very first pulses (Fig. 6b). Already after the first pulse, the transmission of the laser-induced graphitised layer appears to be close to the steady-state level ($T_{gr} \approx 0.1$), around which it oscillates during subsequent irradiation. The lower level of transmission for nanosecond pulses as compared to picosecond ones ($T_{gr} \approx 0.2$) is most probably due to a greater thickness of the graphitised layer. This assumption agrees with the data of Ref. [20], where the mean thickness of the graphitised layer for pulses with $\tau = 20$ ns amounted to nearly 200 nm, against ~40 nm for picosecond and femtosecond pulses. This result was explained by the fact that for nanosecond pulses the distance of heat wave propagation in the material considerably exceeds the radiation absorption depth in the graphitised layer. This fact determines both the leading role of the heat conduction mechanism in the formation of the graphitised layer and the greater thickness of this layer. On the contrary, in the case of ultrashort pulses, the heat transfer from the surface into the material can be neglected and the formation of the graphitised layer in the process of ablation is limited by the depth of radiation absorption.

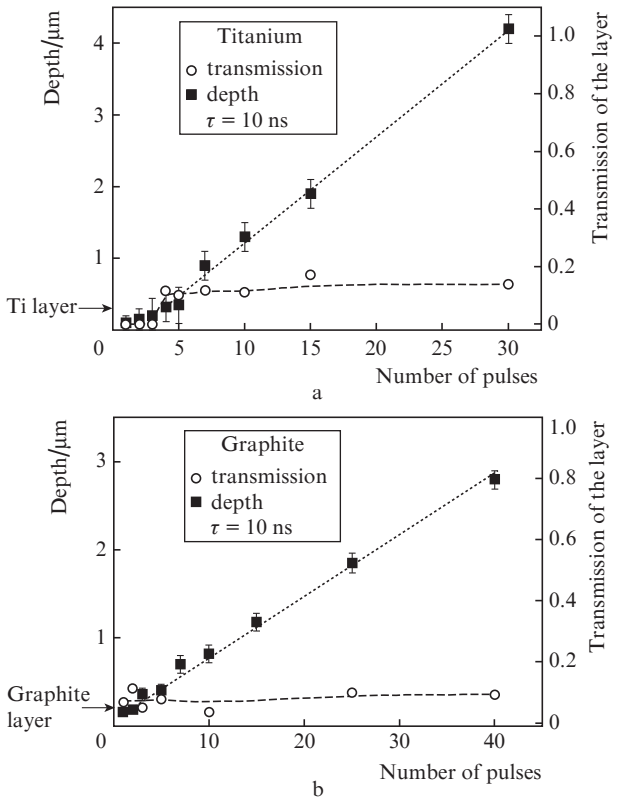

Figure 6. Dependence of the crater depth and the transmission of the graphitised layer ($\lambda = 488$ nm) on the number of pulses under the ablation of diamond with (a) titanium and (b) graphite coatings by the pulses with $\tau = 10$ ns ($F = 4.2$ J cm^{-2}).

3.4. Comparison of regimes

The comparison of the studied regimes of diamond laser ablation, differing in the duration of laser pulses and the nature of the initial absorbing layer could be uncomplete without the data on the rates of the crater depth growth at the linear section (Fig. 7). In combination with the above thorough analysis of the dynamics of crater formation and laser-induced graphitised layer, these data allow the following practical conclusions.

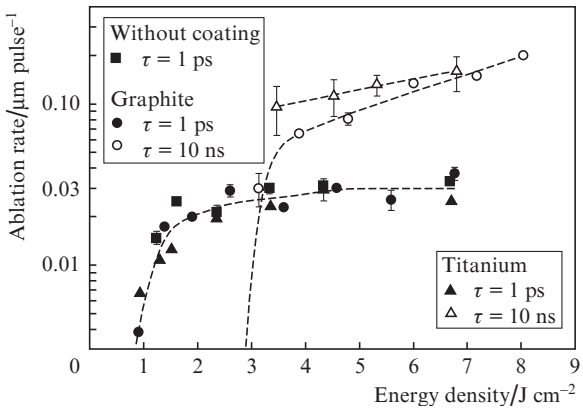

Figure 7. Ablation rates at the linear section of the crater depth growth for different pulse durations and types of initial coating.

1. The deposition of an absorbing layer on the diamond surface practically does not affect the rate of its ablation by picosecond pulses, as well as the minimal energy density necessary for ablation (~1 J cm^{-2}). On the contrary, for nanosecond pulses both tested absorbing coatings decreased the threshold energy density for the initiation of ablation by more than an order of magnitude, from $F_{th} > 40$ J cm^{-2} to $F_{th} \sim 3$ J cm^{-2}.

2. In the presence of an absorbing coating, nanosecond pulses provide the productivity (ablation rate) by nearly 5 times higher than picosecond ones with the same value of the incident energy density.

3. For the diamond microstructuring by picosecond pulses, only the preliminary graphitisation of the diamond surface allows one to avoid the laser-induced breakdown inside the sample because of the fast formation of a self-maintained graphitised layer. However, keeping in mind the relatively high transmission of this layer (by estimates, ~34% for $\lambda = 1030$ nm), the energy density in this case should not strongly exceed the optical breakdown threshold in the diamond volume.

4. The considerable reduction of the ablation threshold mentioned above for nanosecond pulses, when using both titanium and graphite coatings, allows the microstructuring of the diamond surface at the energy densities much lower than the optical breakdown threshold, which ensures the absence

of internal laser-induced damages. Note that although the technology of diamond surface metallisation is simpler and cheaper than the formation of a graphite surface layer, the removal of the metal layer by the first laser pulse from the peripheral region of the laser spot can be a problem in the case of beam scanning over the diamond surface. Therefore, additional studies are necessary to clarify the optimal composition of the initial absorbing layer.

4. Conclusions

We have demonstrated that the preliminary deposition of absorbing layers on the diamond surface is an efficient method of improving the quality and productivity of pulsed laser ablation processing of this material. It is found that the implantation graphitisation of the diamond surface allows one to accelerate the formation of a self-maintaining graphitised layer under irradiation by IR picosecond pulses. When using IR nanosecond pulses, the absorbing coating (both metal and graphite) affects the process of diamond ablation even stronger, decreasing the ablation threshold by more than an order of magnitude. This allows diamond to be processed at energy densities below the optical breakdown threshold, which excludes the laser-induced damage of deep regions of diamond and uncontrolled explosive ablation in the near-surface layer. The obtained results have important practical significance, offering new prospects of using nanosecond lasers for fabricating diamond microstructures.

Acknowledgements. The work was supported by the Russian Science Foundation (Grant No. 14-22-00243).

References

1. Okano K., Hoshina K., Iida M., Koizumi S., Inuzuka T. *Appl. Phys. Lett.*, **64**, 2742 (1994).
2. Ralchenko V.G., Khomich A.V., Baranov A.V., Vlasov I.I., Konov V.I. *Phys. Status Sol. A*, **174**, 171 (1999).
3. Ando Y., Nishibayashi Y., Kobashi K., Hirao T., Oura K. *Diamond Relat. Mater.*, **11**, 824 (2002).
4. Ding G.F., Mao H.P., Cai Y.L., Zhang Y.H., Yao X., Zhao X.L. *Diamond Relat. Mater.*, **14**, 1543 (2005).
5. Wang C.F., Hanson R., Awschalom D.D., Hu E.L., Feygelson T., Yang J., Butler J.E. *Appl. Phys. Lett.*, **91**, 201112 (2007).
6. Karlsson M., Nikolajeff F. *Opt. Express*, **11**, 502 (2003).
7. Gu E., Choi H.W., Liu C., Griffin C., Girkin J.M., Watson I.M., Dawson M.D., McConnell G., Gurney A.M. *Appl. Phys. Lett.*, **84**, 2754 (2004).
8. Lee C.L., Gu E., Dawson M.D. *Diamond Relat. Mater.*, **16**, 944 (2007).
9. Smedley J., Bohon J., Wu Q., Rao T. *J. Appl. Phys.*, **105**, 123107 (2009).
10. Okuchi T., Ohfuji H., Odake S., Kagi H., Nagatomo S., Sugata M., Sumiya H. *Appl. Phys. A*, **96**, 833 (2009).
11. Zalloum O.H.Y., Parrish M., Terekhov A., Hofmeister W. *Opt. Express*, **18**, 13122 (2010).
12. Su S., Li J., Lee G.C.B., Sugden K., Webb D., Ye H. *Appl. Phys. Lett.*, **102**, 231913 (2013).
13. Terentyev S., Blank V., Polyakov S., Zholudev S., Snigirev A., Polikarpov M., Kolodziej T., Qian J., Zhou H., Shvyd'ko Y. *Appl. Phys. Lett.*, **107**, 111108 (2015).
14. Gololobov V.M., Kononenko V.V., Konov V.I. *Quantum Electron.*, **46**, 1154 (2016) [*Kvantovaya Elektron.*, **46**, 1154 (2016)].
15. Kononenko V.V., Gololobov V.M., Pashinin V.P., Konov V.I. *Quantum Electron.*, **46**, 899 (2016) [*Kvantovaya Elektron.*, **46**, 899 (2016)].
16. Johnston C., Chalker P.R., Buckley-Golder I.M., Marsden P.J., Williams S.W. *Diamond Relat. Mater.*, **2**, 829 (1993).
17. Chan S.S.M., Raybould F., Arthur G., Goodall F., Jackman R.B. *Diamond Relat. Mater.*, **5**, 317 (1996).
18. Kononenko V.V., Konov V.I., Pimenov S.M., Prokhorov A.M., Pavel'ev V.S., Soifer V.A. *Quantum Electron.*, **29**, 9 (1999) [*Kvantovaya Elektron.*, **26**, 9 (1999)].
19. Kononenko V.V., Kononenko T.V., Konov V.I., Pimenov S.M., Garnov S.V., Tishchenko A.V., Prokhorov A.M., Khomich A.V. *Quantum Electron.*, **29**, 158 (1999) [*Kvantovaya Elektron.*, **26**, 158 (1999)].
20. Kononenko V.V., Kononenko T.V., Pimenov S.M., Sinyavskii M.N., Konov V.I., Dausinger F. *Quantum Electron.*, **35**, 252 (2005) [*Kvantovaya Elektron.*, **35**, 252 (2005)].
21. Konov V.I. *Laser Photonics Rev.*, **6**, 739 (2012).
22. Kononenko T.V., Meier M., Komlenok M.S., Pimenov S.M., Romano V., Pashinin V.P., Konov V.I. *Appl. Phys. A*, **90**, 645 (2008).
23. Ferrari A.C., Robertson J. *Phys. Rev. B*, **61**, 14095 (2000).
24. Williams M.W., Arakawa E.T. *J. Appl. Phys.*, **43**, 3460 (1972).
25. Pajasova L., Soukup L., Jastrabik L., Chvostova D. *Surf. Rev. Lett.*, **9**, 473 (2002).